

oxidase from *Pseudomonas stutzeri* (11) is also informative. Although the  $cbb_3$  enzyme appears to be closer to cNOR than does  $ba_3$ , similarities in the amino acid sequences of NorB and subunit I of  $cbb_3$  are low (<40%). Regardless, the two proteins exhibit highly similar three-dimensional structures. Specifically, 12 central transmembrane helices are conserved that share a topology of tightly packed helices arranged around a low-spin heme and a binuclear active site (i.e., a heme  $b_3/Fe_B$  or a heme  $a_3/Cu_B$ ). In  $ba_3$ , the active-site heme  $a_3/Cu_B$  center is buried in the hydrophobic core of the enzyme, requiring that both polar ( $H^+$ ,  $e^-$ , and  $H_2O$ ) and lipophilic ( $O_2$ ) reactants move along structurally specified pathways to their intended destinations. In cNOR, the active-site heme  $b_3/Fe_B$  is found essentially at the same location in the hydrophobic core. The three histidine side chains that coordinate the  $Cu_B$  in HCO are conserved in cNOR and are supplemented with a glutamyl carboxylate group, providing a favorable coordination shell for an iron ion at the  $Fe_B$  site.

The structure of cNOR also shows that transmembrane pathways (D- and K-paths) for proton uptake are absent; this supports previous findings that cNOR does not pump protons (12) and sheds light on how heme-Cu oxidases acts as a proton pump. Hino *et al.* also propose pathways for electron transfer from the cytochrome c via the low-spin heme

and proton entries from the periplasmic side to the binuclear center. As in  $cbb_3$ , a  $Ca^{2+}$  ion bridges and may stabilize an efficient electron transfer route between the two hemes in NorB. Another remarkable feature of the cNOR structure is the presence of a Y-shaped hydrophobic channel similar to that reported by Luna *et al.* (13) in  $ba_3$  and by Buschmann *et al.* (11) in  $cbb_3$ . In cNOR, this channel must serve to carry NO from the lipid bilayer to the active site.

The authors do not assign the exit route of the  $N_2O$  product, but the factor of 10 increase in water solubility of  $N_2O$  relative to  $O_2$  or NO may allow this small molecule to diffuse through both hydrophobic and hydrophilic channels. A question worthy of future investigation is whether the exit route of  $N_2O$  from cNOR influences its capture by the periplasmic, copper-containing  $N_2O$  reductase, and its escape into the atmosphere. The structure also leaves two other questions unanswered: (i) How do the two NO molecules bind at the diiron site? (ii) How do the N-N bond formation and N-O bond cleavage occur? A distal glutamic acid within 5 Å of the iron cluster that appears conserved in NorB sequences may provide a proton to a putative hyponitrite anion ( $N_2O_2^{2-}$ ) and facilitate N-O bond cleavage. Although most investigators might agree that the first NO binds to the ferrous heme  $b_3$ , the mode of addition of a second NO to this mononitrosyl complex remains to be defined,

as do the respective roles of the two Fe ions (14). Bioengineering models of the heme  $b_3/Fe_B$  site in the simpler protein scaffold of myoglobin will be valuable tools for conducting these mechanistic investigations (15). Structural characterization of other transmembrane NORs in parallel with HCOs will further clarify evolutionary variation in  $Fe_B/Cu_B$  coordination spheres, electron and proton transfer pathways, and hydrophobic channels to the catalytic dinuclear center.

#### References

1. T. Hino *et al.*, *Science* **330**, 1666 (2010); 10.1126/science.1195591.
2. D. E. Canfield, A. N. Glazer, P. G. Falkowski, *Science* **330**, 192 (2010).
3. A. A. Lacin, G. A. Schmidt, D. Rind, R. A. Ruedy, *Science* **330**, 356 (2010).
4. A. Mosier *et al.*, *Nutr. Cycl. Agroecosyst.* **52**, 225 (1998).
5. N. Barraud *et al.*, *J. Bacteriol.* **188**, 7344 (2006).
6. T. Romeo, *J. Bacteriol.* **188**, 7325 (2006).
7. T. M. Stevanin, J. R. Laver, R. K. Poole, J. W. B. Moir, R. C. Read, *Microbes Infect.* **9**, 981 (2007).
8. M. M. Pereira, M. Santana, M. Teixeira, *Biochim. Biophys. Acta* **1505**, 185 (2001).
9. S. de Vries, I. Schröder, *Biochem. Soc. Trans.* **30**, 662 (2002).
10. L. M. Hunsicker-Wang, R. L. Pacoma, Y. Chen, J. A. Fee, C. D. Stout, *Acta Crystallogr. D.* **61**, 340 (2005).
11. S. Buschmann *et al.*, *Science* **329**, 327 (2010).
12. U. Flock *et al.*, *J. Biol. Chem.* **238**, 3839 (2008).
13. V. M. M. Luna, Y. Chen, J. A. Fee, C. D. Stout, *Biochemistry* **47**, 4657 (2008).
14. P. Moëne-Loccoz, *Nat. Prod. Rep.* **24**, 610 (2007).
15. N. Yeung *et al.*, *Nature* **462**, 1079 (2009).

10.1126/science.1200247

## MATERIALS SCIENCE

# Optical Metamaterials— More Bulky and Less Lossy

Costas M. Soukoulis<sup>1,2</sup> and Martin Wegener<sup>3</sup>

Usually, investigators in materials science have asked: “What properties does a certain new material or structure have?” Now, the inverse problem arises: “I want to achieve certain—possibly unheard-of—material properties. How should the corresponding micro- or nanostructure look?” Examples could be: efficiently blocking acoustic noise due to a

highway from a nearby village by a tailored wall, concentrating electromagnetic energy into as-tight-as-possible spaces, or avoiding reflections from a material’s surface. The underlying common scheme is wave physics. Material properties that were otherwise unachievable, e.g., negative refraction and cloaking, may eventually be designed into optical metamaterials and photonic crystals. Both require tailoring of the properties (i.e., phase velocity and impedance) of an electromagnetic wave moving through the substance at the local level. In photonic crystals, the phase velocity of an electromagnetic wave moving through the crystal is controlled by tuning the photonic band structure; the impedance is determined

Advanced techniques for bulk fabrication and loss reduction provide good prospects for practical optical metamaterials.

by the electromagnetic field distributions throughout the material. In metamaterials, this amounts to tailoring the effective electric permittivity and magnetic permeability. In either case, introducing resonances is the key to controlling the local wave properties. The recent development of advanced fabrication techniques being applied to metamaterials and photonic crystals may lead to realization of such designer materials.

In photonic crystals, the focus has traditionally been on many wavelength-scale building blocks arranged on a dielectric lattice (generalized Bragg resonances) that produce collective resonances in response to an electromagnetic field, whereas researchers working with metamaterials started with

<sup>1</sup>Ames Laboratory and Department of Physics and Astronomy, Iowa State University, Ames, IA 50011, USA. <sup>2</sup>Institute of Electronic Structure and Laser—Foundation for Research and Technology Hellas, University of Crete, Heraklion, Crete, Greece. <sup>3</sup>Institute of Applied Physics, Institute of Nanotechnology, and Center for Functional Nanostructures, Karlsruhe Institute of Technology, Karlsruhe, Germany. E-mail: soukoulis@ameslab.gov

densely packed, ideally noninteracting resonances of individual subwavelength-size building blocks (generalized Mie resonances). Mie resonances are especially pronounced for metals. In general, both Bragg- and Mie-type resonances are advantageous.

In 2007, optical metamaterials (1) were not actually “materials” but were rather metafilms or metasurfaces—planar monolayers of meta-atoms. Today, various truly three-dimensional (3D) optical metamaterial structures have been reported (see the figure) (2–5). The larger the 3D metal-based metamaterial structures become and the more the “bulk” is approached, the more obvious it becomes that losses must be reduced. Otherwise, a large chunk of metamaterial

will simply be black and opaque, rendering it useless. At optical frequencies, most of the losses result from the constituent metal. Thus, avoiding sharp edges for the current flow and/or avoiding nearby resonances can eliminate part of the losses. Superconductors may appear as a remedy for resistive losses, but their small superconducting band-gap frequency inherently prohibits operation at optical or even visible frequencies.

A different approach to reduce losses is to incorporate active gain materials to counteract the losses and achieve negative phase velocities of light. The fact that we are unable to change the past strongly connects losses and phase velocities of light. Combined with the condition of stability, this

imposes rather stringent fundamental constraints on what is possible—regardless of the particular design (6, 7). As in any laser, the system becomes intrinsically unstable for macroscopic metamaterial structures and for long times even if the gain exceeds the loss only at a single frequency. Thus, the effective loss can only be zero at a single frequency, for which the phase velocity of light may be negative. For all other frequencies, the losses remain finite. Spontaneous and stimulated emissions will occur and must be considered as intense sources of “noise” if the artificial material shall be used to guide, focus, and/or influence external light. This aspect might force a retraction from the exact gain-equals-loss condition, leaving behind losses that can still be orders of magnitude lower compared to those in the absence of gain material.

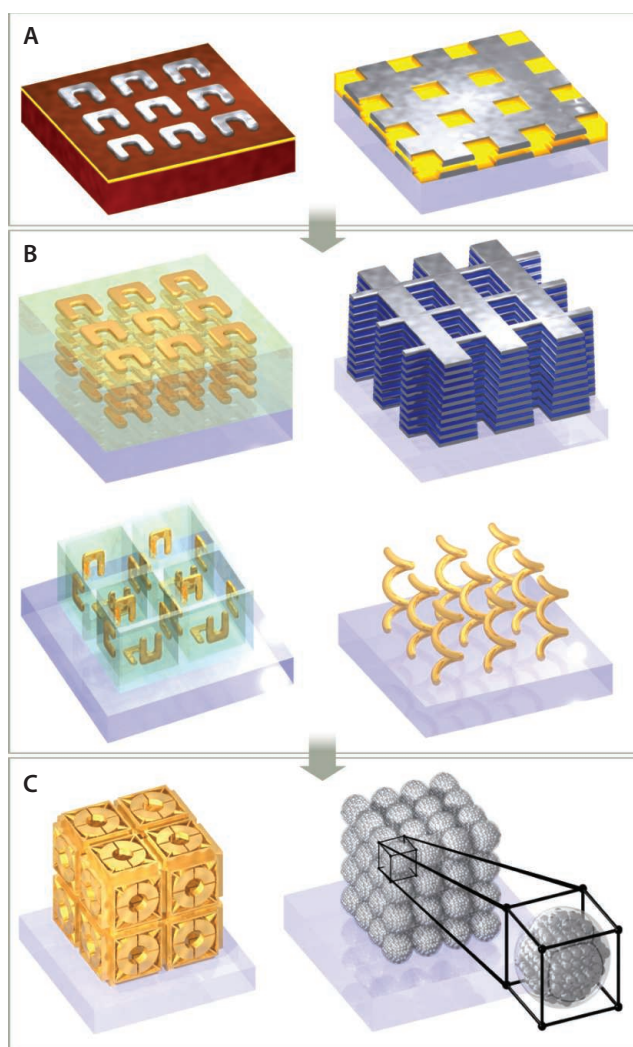
Recent experiments on gain have returned to metafilms to avoid tackling both the bulk and the loss challenges simultaneously. Only partial loss compensation has been obtained in exper-

iments with quantum dots (8) and single quantum wells (9), whereas it was possible to compensate for losses completely in the visible range via dyes embedded in epoxy resin and pumped by picosecond pulses (10). The latter experiment and corresponding theory (11, 12) have raised hopes, but it is not clear that this success can be translated to macroscopic 3D photonic metamaterials under steady-state conditions.

Three crucial aspects have already been demonstrated experimentally: (i) operation in the visible spectrum, (ii) truly 3D optical metamaterials, and (iii) loss-free metamaterials. Another crucial aspect for many applications that has only been achieved theoretically so far is isotropy (13, 14). Realizing the ideal negative-index metamaterials, i.e., a 3D isotropic zero-loss negative-index metamaterials operating at visible wavelengths, requires the combination of all these aspects. It is unlikely that compensating loss via optical pumping will meet real-world requirements, whereas injecting an electrical current into a semiconductor through two wires coming out of a chunk of metamaterial is more practical. Once all of this has been achieved, the next frontier toward commercialization is bringing the fabrication cost down, e.g., with nanochemistry-based bottom-up self-assembly approaches (13). Another interesting though unexplored avenue is replacing the lithographically defined meta-atoms by tailored large molecules. Ideally, these molecules could be assembled to 3D molecular crystals.

#### References and Notes

1. C. M. Soukoulis, S. Linden, M. Wegener, *Science* **315**, 47 (2007).
2. N. Liu *et al.*, *Nat. Mater.* **7**, 31 (2008).
3. J. Valentine *et al.*, *Nature* **455**, 376 (2008).
4. J. K. Gansel *et al.*, *Science* **325**, 1513 (2009).
5. D. B. Burckel *et al.*, *Adv. Mater.* **22**, 3171 (2010).
6. M. I. Stockman, *Phys. Rev. Lett.* **98**, 177404 (2007).
7. P. Kinsler, M. W. McCall, *Phys. Rev. Lett.* **101**, 167401 (2008).
8. E. Plum, V. A. Fedotov, P. Kuo, D. P. Tsai, N. I. Zheludev, *Opt. Express* **17**, 8548 (2009).
9. N. Meinzer *et al.*, *Opt. Express* **18**, 24140 (2010).
10. S. Xiao *et al.*, *Nature* **466**, 735 (2010).
11. S. Wuestner, A. Pusch, K. L. Tsakmakidis, J. M. Hamm, O. Hess, *Phys. Rev. Lett.* **105**, 127401 (2010).
12. A. Fang, Th. Koschny, C. M. Soukoulis, *Phys. Rev. B* **82**, 121102 (2010).
13. C. Rockstuhl, F. Lederer, C. Etrich, T. Pertsch, T. Scharf, *Phys. Rev. Lett.* **99**, 017401 (2007).
14. D. O. Güney, T. Koschny, C. M. Soukoulis, *Opt. Express* **18**, 12348 (2010).
15. We thank M. Decker for preparing the figure. Supported by the European Union FET project PHOME (contract 213390); by Ames Laboratory, U.S. Department of Energy (Basic Energy Sciences), under contract DE-AC02-07CH11358; by Office of Naval Research and Air Force Office of Scientific Research—Multidisciplinary University Research Initiative grants (C.M.S.); and by projects CFN A1.5 and METAMAT (M.W.).



**Bulking up.** Metamaterials operating at optical frequencies have developed from planar monolayers of meta-atoms (A) to truly 3D nanostructures (2–5). Incorporating gain materials (yellow in top box) led to loss reduction (8–10). (C) Blueprints for isotropic metamaterials based on bottom-up self-assembly (13) or direct laser writing (14) do exist. If all of these aspects could be combined, one of the early dreams of the field, namely, visible 3D isotropic zero-loss negative-index metamaterials, might eventually become reality.